NGI Technical note

To:	Norges vassdrags- og energidirektorat (NVE)
Attn.:	Odd Are Jensen
Copy to:	CJ, PG, CTr, HVi, SGl, UD, HHH
Date:	2023-08-24
Revision no./Rev.date:	0/
Document no.:	20200017-10-TN
Project:	Applied Avalanche Research in Norway (AARN)
Project manager:	Kjersti G. Gisnås
Prepared by:	Dieter Issler
Reviewed by:	Hervé Vicari

Outline of a Simple Model of Mixed Snow Avalanches

Abstract

This Note discusses a quasi-three-dimensional model of mixed snow avalanches that could replace the code MoT-Voellmy in NAKSIN. As a starting point, the two-layer model by Eglit is slightly simplified and extended from a profile line to a general topography in three-dimensional space. Possible modifications of the closures proposed by Eglit are discussed. For rapid development, it is suggested to base the new code either on MoT-Voellmy or possibly on the code development system ExaHyPE.

Contents

NORWEGIAN GEOTECHNICAL INSTITUTE
NGI.NO

Main office
PO Box 3930 Ullevaal St.
NO-0806 Oslo
Norway

Trondheim office
PO Box 5687 Torgarden
NO-7485 Trondheim
Norway

T 22 02 30 00
F 22 23 04 48
NGI@ngi.no

BIC NO. DNBANOKK
IBAN NO26 5096 05 01281
ORGANISATION NO.
958 254 318MVA

ISO 9001/14001
CERTIFIED BY BSI
FS 32989/EMS 612006

1 Introduction

NGI has been contracted by the Norwegian Army's Operational Headquarters to produce new avalanche hazard indication maps as an important tool for safe operations in avalanche-prone terrain. These maps are generated semi-automatically by the system NAKSIN (**N**ye **A**ktsomhets**K**art for **S**nøskred **I** **N**orge) (Issler *et al.*, 2020). A key part of NAKSIN is the dynamical run-out model that is used to calculate the area hit by an avalanche of given release area and release depth. So far, the quasi-three-dimensional code MoT-Voellmy, developed at NGI, has been used because of its speed and the availability of the source code.

A significant shortcoming of NAKSIN is that MoT-Voellmy implements the friction law first proposed by Voellmy (1955) and thus accounts only for the dense and fluidized parts of snow avalanches but not for the suspension layer that is generated by medium-to-large-size avalanches and that can run much farther under suitable conditions. The pressure exerted by this powder-snow cloud (PSC) is much weaker (a few kPa or a few tens of kPa in the case of very large events under cold snow conditions) than the one in the dense part, which may reach the MPa range in extreme cases. Nevertheless, these pressures are harmful for persons in open terrain, may cause extended damage to forests, and can even displace large vehicles (there are reports on persons having been carried several hundred meters through the air by the PSC). It has therefore been a strong wish to account for the PSC in the hazard indication maps both for military and civilian use.

There is, however, presently no physically sound and numerically efficient model that can calculate both the dense and dilute parts of snow avalanches in a way that is compatible with NAKSIN. There are a few mass-point models for the PSC only (Kulikovskiy & Sveshnikova, 1977; Fukushima & Parker, 1990; Beghin & Olagne, 1991; Gauer, 1994; Rastello & Hopfinger, 2004; Turnbull *et al.*, 2007), but neither can they easily be adapted to three-dimensional terrain, nor can they incorporate the crucial interaction with the dense core of the avalanche. There are also two models coupling a 3D calculation of the PSC to a quasi-three-dimensional (i.e., depth-averaged) model of the dense core (Naaim & Gurer, 1998; Sampl & Zwinger, 2004). The decisive draw-back of this approach for the present purpose is the computational effort, which is two to three orders of magnitude larger than practical.

A feasible compromise would be a two-layer model, utilizing depth-averaging both in the lower (dense-flow) and upper (suspension-flow) layer. Two such codes have been developed in the past: the earliest two-layer continuum model of mixed snow avalanches by Eglit (1983) and Nazarov (1991), which is quasi-2D, and the recent extension of the commercial code RAMMS::AVALANCHE to fluidizing flows with a suspension layer (Bartelt *et al.*, 2016). The design of the latter (quasi-3D, ESRI ASCII Grid raster files as input) is similar to MoT-Voellmy and well suited for NAKSIN, and the computation times are (marginally) acceptable. However, the program is not officially released, the source code not available, and there are serious flaws in the physical and mathematical formulation of the model (Issler *et al.*, 2018). This makes RAMMS::EXTENDED

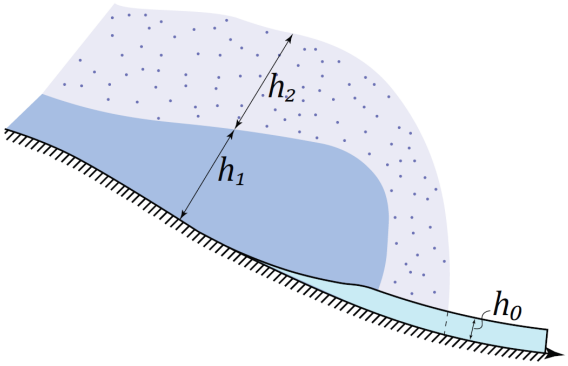

Figure 1 Schematic of Eglit's two-layer model for mixed avalanches. The index 0 refers to the (erodible) snow cover, 1 to the dense flow, and 2 to the powder-snow cloud. From (Eglit et al.*, 2020, Fig. 9)*

unsuitable for the present purpose.

In the following, we summarize and slightly simplify Eglit's model, extend it to a quasi-3D setting, and discuss possible modifications of certain closure assumptions (Sec. 2). On that basis, we compare two opposite approaches to model programming: using MoT-Voellmy as a starting point and adding further partial differential equations (PDEs) for the PSC and new source terms vs. the much more complex but very flexible and extensible model-building environment ExaHyPE (Reinarz *et al.*, 2020), which holds promise of accelerating code creation and can make use of adaptive mesh refinement and other advanced methods (Sec. 3). Based on this, recommendations are given in Sec. 4.

2 Eglit's two-layer model

2.1 Geometrical setting

Eglit's two-layer model is formulated in a curvilinear orthogonal coordinate system (s, z) in a two-dimensional vertical plane. The curve $(s, z = 0)$ is the avalanche path profile; s is the distance along it, z is everywhere normal to the topography. The (erodible) snow cover has initial depth $h_{0,0}(s) = h_0(s, 0)$, the released slab is described by $h_{1,0}(s) = h_1(s, 0)$, and analogously for the powder-snow cloud, which will usually be assumed to be created by the moving avalanche, i.e., $h_{2,0}(s) = h_2(s, 0) = 0$. The densities of the snow cover and dense flow are assumed constant at ρ_0 and ρ_1, respectively. The (depth-averaged) density of the PSC, ρ_2, varies in space and time.

To extend this model to a 2D curved surface embedded in 3D Euclidean space is not as trivial as it might appear at first sight. In the 1D (i.e., quasi-2D) case, the arc length parameterizes the profile curve in a suitable way. An orthogonal coordinate system is

easily constructed by choosing the z coordinate lines as straight lines crossing the path profile ($z = 0$) at a right angle. It has been known for a long time how to account for path curvature (Eglit, 1983). On a curved surface, however, one cannot in general construct an orthonormal coordinate system. Probably the simplest solution for practical purposes—well suited for codes to be used in a GIS context—is to start from a 3D Cartesian coordinate system (X, Y, Z), within which the topography Σ is described by a function $Z(X, Y)$ (typically given on a regular grid). This induces a *curvilinear* coordinate system (x, y) on Σ, in which the point P with Cartesian coordinates $(X, Y, Z(X, Y))$ has (local) coordinates $x = X, y = Y, z = 0$). To derive the model equations, one needs to extend this coordinate system into a three-dimensional one; it is useful to choose straight z coordinate lines that are perpendicular to Σ.

For a derivation of an explicitly covariant formulation of the balance equations, see (Issler, 2006). However, for the present purposes only the dominant effects of curvature will be retained, namely centrifugal forces and the expression for the length of a vector in a non-orthogonal coordinate system, i.e., $\|\boldsymbol{a}\| = (a_x^2 + a_y^2 + 2a_x a_y \cos\alpha)^{1/2}$, with α the angle between the tangent vectors to the x and y-coordinate lines at the given point. There are two alternative formulations of the model on the curved surface. The first is to use the computational coordinates, relative to which the grid spacing is uniform, and use the metric tensor at the surface Σ,

$$\boldsymbol{G}(x, y, z = 0) = \begin{pmatrix} 1 + (\partial_X Z)^2 & (\partial_X Z)(\partial_Y Z) \\ (\partial_X Z)(\partial_Y Z) & 1 + (\partial_Y Z)^2 \end{pmatrix}, \tag{1}$$

explicitly in the PDEs. In the second alternative, one measures distances and velocities in physical units and takes into account that the grid is neither uniform nor orthogonal in these coordinates. One finds

$$\Delta x = \sqrt{1 + (\partial_X Z)^2}\,\Delta X \tag{2}$$

$$\Delta y = \sqrt{1 + (\partial_Y Z)^2}\,\Delta Y \tag{3}$$

for the side lengths of the cells,

$$\Delta A = \sqrt{\det(\boldsymbol{G})}\,\Delta X \Delta Y = \sqrt{1 + (\partial_X Z)^2 + (\partial_Y Z)^2}\,\Delta X \Delta Y \tag{4}$$

for the area of a cell, and

$$(\mathrm{d}\boldsymbol{v})^2 = v_x^2 + v_y^2 + 2v_x v_y \frac{(\partial_X Z)(\partial_Y Z)}{\sqrt{[1 + (\partial_X Z)^2][1 + (\partial_Y Z)^2]}} \tag{5}$$

for the length of a vector $\boldsymbol{v}$, the components of which are expressed in *physical* units. The code MoT-Voellmy, which could serve as a starting point for the present numerical model (Sec. 3), implements the latter approach.

2.2 Basic modeling assumptions

Eglit's model represents a minimal system for a continuum description of mixed snow avalanches if one wishes to include the following physical effects:

- Avalanches exhibit (at least) two flow regimes with distinct physical properties that may coexist—a dense core following the terrain and a dilute suspension layer overlying and often also preceding the core. The densities of both layers can vary in space and time. Observations and experiments reveal that there is an intermediate flow regime (variably called "light flow", "saltation layer", "fluidized flow", "intermittent flow"), which contains both large particles and fine snow grains. It shares more properties with the dense core than with the suspension layer and can, in principle, be captured by specifying an appropriate rheology for a dense to semi-dilute granular medium (see, e.g., Issler & Gauer, 2008, and references therein).
- Only depth-averaged values of the physical variables are computed directly (their dependence on the z-coordinate may be approximated after the computation of the depth-averaged values).
- The mass of the interstitial air can be safely neglected in the dense layer but not in the PSC.
- The avalanche may entrain mass from the snow cover and lose mass at its surface due to drag, thus creating and nurturing a PSC. Some of this mass may return to the dense layer if particles settle out of the PSC.
- The PSC entrains ambient air by turbulent mixing along its surface.
- If the PSC separates from the dense flow, it may entrain snow from the snow cover and/or deposit mass onto it.

These properties are well confirmed by observations and experiments and capture most of the practically relevant features of mixed snow avalanches.

One characteristic feature of the PSC is not explicitly listed above, namely the essential role of *turbulence*, which keeps the particles in suspension over an extended period. Another practically important consequence of turbulence is that the instantaneous pressure can be much larger than the pressure averaged over time intervals corresponding to large eddies and that the flow direction fluctuates wildly. The balance between production and dissipation of turbulence is decisive for the evolution of the PSC; Parker *et al.* (1986) demonstrate this clearly for turbidity currents by comparing two variants of their model, one with empirical, algebraic closure assumptions for turbulent quantities and one with a balance equation for turbulent kinetic energy K. At this point, we follow Eglit's ansatz and do not include a balance equation for K, but this option should be explored at a later stage.

Another (preliminary) simplification we make is to assume constant density in the lower layer. This has the advantages of reducing the number of balance equations by one and allowing to make direct contact with traditional dense-flow models. However, at a later stage it will be highly desirable to allow flow-regime transitions in the denser layer.

2.3 Mathematical formulation

If entrainment of the snow cover is included, a minimum of 6 PDEs is required in 1D, and 8 in 2D. We extend the equations presented by Eglit *et al.* (2020) to the 2D case and allow for a density difference between the snow cover (ρ_0) and the dense flow (ρ_1) but assume $\rho_1 = \text{cst.}$. They can be written as an Exner equation for the snow cover,

$$\rho_0 \partial_t h_0 = -q_{01} - q_{02} + q_{10} + q_{20}, \tag{6}$$

mass and momentum balances for the dense-flow part,

$$\partial_t(\rho_1 h_1) + \boldsymbol{\nabla}_{\|} \cdot (\rho_1 h_1 \boldsymbol{u}_1) = q_{01} - q_{10} - q_{12} + q_{21}, \tag{7}$$

$$\begin{aligned} \partial_t(\rho_1 h_1 \boldsymbol{u}_1) + \boldsymbol{\nabla}_{\|} \cdot (\rho_1 h_1 \boldsymbol{u}_1 \boldsymbol{u}_1) + \boldsymbol{\nabla}_{\|} \left(\tfrac{1}{2}\rho_1 g_z h_1^2\right) \\ = \rho_1 h_1 [\boldsymbol{g}_{\|} - \boldsymbol{\nabla}_{\|}(g_z h_0)] - h_1 \boldsymbol{\nabla}_{\|}(\rho_2 h_2 g_z) \\ + \boldsymbol{\tau}_{21} - \boldsymbol{\tau}_{10} - q_{12}\boldsymbol{u}_1 + q_{21}\boldsymbol{u}_2, \end{aligned} \tag{8}$$

and volume, mass and momentum balances for the PSC,

$$\partial_t h_2 + \boldsymbol{\nabla}_{\|} \cdot (h_2 \boldsymbol{u}_2) = \frac{q_{02} - q_{20}}{\rho_0} + \frac{q_{12} - q_{21}}{\rho_1} + \frac{q_{a2}}{\rho_a}, \tag{9}$$

$$\partial_t(\rho_2 h_2) + \boldsymbol{\nabla}_{\|} \cdot (\rho_2 h_2 \boldsymbol{u}_2) = q_{02} - q_{20} + q_{12} - q_{21} + q_{a2}, \tag{10}$$

$$\begin{aligned} \partial_t(\rho_2 h_2 \boldsymbol{u}_2) + \boldsymbol{\nabla}_{\|} \cdot (\rho_2 h_2 \boldsymbol{u}_2 \boldsymbol{u}_2) + \boldsymbol{\nabla}_{\|} \left(\tfrac{1}{2}(\rho_2 - \rho_a) g_z h_2^2\right) \\ = (\rho_2 - \rho_a) h_2 [\boldsymbol{g}_{\|} - \boldsymbol{\nabla}_{\|}(g_z(h_0 + h_1))] \\ + \boldsymbol{\tau}_{a2} - \boldsymbol{\tau}_{20} - \boldsymbol{\tau}_{21} + q_{12}\boldsymbol{u}_1 - (q_{20} + q_{21})\boldsymbol{u}_2. \end{aligned} \tag{11}$$

In these equations, $\boldsymbol{\nabla}_{\|}$ and $\boldsymbol{g}_{\|}$ are the components of the gradient operator and the gravitational acceleration confined to the local tangent plane. The index a refers to the ambient air. In the entrainment (or mass-exchange) fluxes q_{ij}, the index i indicates the layer of origin, j the target layer—opposite to the notation in (Eglit, 1983; Eglit *et al.*, 2020). The sign of the interfacial shear stresses is positive if the upper layer drags the lower one in the coordinate direction.

In Eqs. (6)–(11), some misprints in (Eglit *et al.*, 2020) have been corrected, in agreement with (Eglit, 1983). The notation has been modified slightly by using entrainment *rates* rather than entrainment *velocities* to emphasize the numerical equality of corresponding terms in Eqs. (6), (7), (9) and (10), and in Eqs. (8) and (11). The equations have also been arranged so that the left-hand side only contains time derivatives and divergences of (depth-integrated) fluxes while other derivative terms are on the right-hand side together with the source terms. More importantly, the density of layer 1 is here assumed constant to reduce the computational effort, facilitate comparison with traditional one-layer models of the Voellmy type, and to dodge the question of how the friction coefficients depend on the density (Issler & Gauer, 2008).

Equation (9) represents volume conservation in a mixture of incompressible components. This does not preclude the suspension-layer density ρ_2 from changing because the volume concentration of snow grains changes due to air entrainment at the upper surface and snow entrainment at the bottom of the layer. When snow is suspended from the snow cover, both the ice and the interstitial air are entrained; accordingly, the volume influx is q_{02}/ρ_0, and similarly for entrainment from the denser part of the flow. As particles settle out of the suspension layer, they trap some air between themselves; for simplicity, we assume the deposit to have the same density as its target layer.

The last terms on the last line of Eq. (11) quantify the momentum exchange between layers induced by mass exchange. This momentum flux is given by the product of the mass flux and the (slope-parallel) velocity at the interface, which in general is different from the mean velocities in either layer. The velocities associated with q_{01} and q_{02} vanish, and according to the results of Rauter & Köhler (2020) one may also assume this for deposition from the lower avalanche layer (q_{10}). The velocity at the interface between the dense and suspension layer at $z = z_i$ is expected to be between $\boldsymbol{u}_1$ and $\boldsymbol{u}_2$, Eglit (1983) chose $\boldsymbol{u}_2$, but if one considers the dense layer to exhibit little shearing except near the bottom, $\boldsymbol{u}_1$ might be a better approximation. If the model is extended slightly by prescribing specific shapes for the velocity profiles, the constraint $\boldsymbol{u}_1(z_i) = \boldsymbol{u}_2(z_i)$ applies and the velocity at the interface can be expressed in terms of $\boldsymbol{u}_1$ or $\boldsymbol{u}_2$.

2.4 Closure assumptions

To completely specify the model, closure relations for the four shear stresses $\boldsymbol{\tau}_{10}$, $\boldsymbol{\tau}_{20}$, $\boldsymbol{\tau}_{21}$ and $\boldsymbol{\tau}_{a2}$ and the six mass exchange rates q_{01}, q_{02}, q_{12}, q_{20}, q_{21} and q_{a2} must be given. (In view of the findings of Rauter & Köhler (2020), one may consider adding a deposition rate from the dense flow, q_{10}.)

Shear stresses In the original model MSU-1 (Eglit, 1983, 1998), the shear stress $\boldsymbol{\tau}_{01}$ is specified as the sum of Coulomb friction limited to a material-dependent maximum shear strength $\tau_{\max}$ according to a proposal by Grigoryan (1979) and the well-known Voellmy drag term:

$$\boldsymbol{\tau}_{10} = \frac{\boldsymbol{u}_1}{\|\boldsymbol{u}_1\|}\left[\max(\mu\sigma_{zz}, \tau_{\max}) + k\rho_1\boldsymbol{u}_1^2\right]. \tag{12}$$

(If the flow is at rest, the bed shear stress is limited by the gravitational traction minus the pressure gradient.) The limitation of Coulomb friction is empirical but has the desirable effect that very deep avalanches have longer run-out than shallow ones. We will here disregard Eglit's (1983) proposal, in which viscous drag proportional to $\|\boldsymbol{u}_1\|$ replaces the "turbulent" drag proportional to $\|\boldsymbol{u}_1\|^2$ if the Reynolds number is below a critical value. The normal stress at the snow-cover–avalanche interface acquires a contribution due to the weight of the PSC:

$$\sigma_{zz} = g_z'\left[\rho_1 h_1 + (\rho_2 - \rho_a)h_2\right]. \tag{13}$$

If one wishes to account for the dominant curvature effects, $g_z' \approx g\cos\theta + \kappa_{\boldsymbol{u}_1}\boldsymbol{u}_1^2$, with θ the local slope angle and $\kappa_{\boldsymbol{u}_1}$ the terrain curvature in the flow direction.

The drag at the bottom of a dilute turbulent flow like a (low-density) turbidity current, dilute pyroclastic flow (nuage ardente) or PSC is often considered negligible compared to the effect of entrainment of ambient fluid across its upper surface. However, this may not be so in the case of flows with bottom density much larger than the ambient-fluid density ρ_a, high shear rates at the bottom and a rough surface—all these conditions apply to PSCs. Eglit (1983) proposes an expression for $\boldsymbol{\tau}_{20}$ and $\boldsymbol{\tau}_{21}$ based on formulas for the drag in fluid flows over a rough surface. The main differences between drag of the PSC against the dense flow and the snow cover are (i) the relative velocity, $\boldsymbol{v}$, which equals $\boldsymbol{u}_2$ for the snow cover and $\boldsymbol{u}_2 - \boldsymbol{u}_1$ for the dense flow, and (ii) the drag coefficient, which is expected to be substantially larger on the surface of the dense flow, where the aerodynamic roughness length is of the order of 0.1 m against 0.001 m on the snow cover. However, there is probably an important contribution from snow grains impacting the surface as well. One may thus write

$$\boldsymbol{\tau}_{2i} = C_{d,i}\rho_2\|\boldsymbol{v}_i\|\,\boldsymbol{v}_i, \tag{14}$$

where the index i is 0 for the snow cover and 1 for the dense flow. The drag coefficients $C_{d,i}$ may also include a factor accounting for the ratio between the concentration at the bottom of the PSC and the depth-averaged value of ρ_2. At any rate, the $C_{d,i}$ must be considered empirical parameters at this stage; for indications of their values, see the references in (Eglit *et al.*, 2020, Sec. 5). Also see (Sampl & Zwinger, 2004) for an attempt to fix the parameters of a similar drag model using boundary-layer theory.

The Eglit model contains an air-entrainment term q_{a2} in the PSC mass balance, which leads to an entrainment-induced deceleration term $-q_{a2}\|\boldsymbol{u}_2-\boldsymbol{u}_a\|(\boldsymbol{u}_2-\boldsymbol{u}_a)$ in the equation of motion (as opposed to the momentum balance equation), *and* an explicit shear-stress term $\boldsymbol{\tau}_{a2}$ due to the shearing of the PSC against the ambient air. There appears to be some uncertainty whether both terms are needed or only the entrainment term. This can be answered by applying Reynolds-averaging to the (depth-resolved) mass balance and the Navier–Stokes equation. In this formalism, the fields are written as the sum of their averaged and fluctuation values, $\Phi(\boldsymbol{x},t) = \bar{\Phi}(\boldsymbol{x},t) + \Phi'(\boldsymbol{x},t)$, where the averaging time is assumed short relative to the inverse frequency of the macroscopically relevant modes. It follows that $\overline{\Phi'} = 0$. In the present case, with both snow particles and air assumed incompressible, the instantaneous density is decomposed as

$$\rho = \rho_a + c\Delta\rho = [\rho_a + \bar{c}\Delta\rho] + c'\Delta\rho = \bar{\rho} + \rho', \tag{15}$$

where c is the volumetric concentration of snow particles of intrinsic density $\rho_p = \rho_a + \Delta\rho$. Time averaging the mass conservation equation of the mixture, $\partial_t\bar{\rho} + \boldsymbol{\nabla}\cdot(\overline{\rho\boldsymbol{u}}) = 0$, leads to

$$\partial_t\bar{\rho} + \boldsymbol{\nabla}\cdot(\bar{\rho}\bar{\boldsymbol{u}}) = -\Delta\rho\boldsymbol{\nabla}\cdot(\overline{c'\boldsymbol{u}'}).$$

Closure assumptions are needed for the right-hand side, typically using the mixing-length hypothesis, which leads to

$$-\Delta\rho\boldsymbol{\nabla}\cdot(\overline{c'\boldsymbol{u}'}) \approx -\Delta\rho\boldsymbol{\nabla}\cdot(-D_t\boldsymbol{\nabla}\bar{c}) = \boldsymbol{\nabla}\cdot(D_t\boldsymbol{\nabla}\bar{\rho}). \tag{16}$$

with D_t the turbulent diffusion constant for (snow) mass. The Reynolds-averaged Navier–Stokes (RANS) equation is

$$\partial_t(\bar{\rho}\bar{\boldsymbol{u}} + \overline{\rho'\boldsymbol{u}'}) + \boldsymbol{\nabla}\cdot(\bar{\rho}\bar{\boldsymbol{u}}\bar{\boldsymbol{u}} + \bar{\rho}\overline{\boldsymbol{u}'\boldsymbol{u}'} + \overline{\rho'\boldsymbol{u}'}\bar{\boldsymbol{u}} + \overline{\rho'\boldsymbol{u}'}\bar{\boldsymbol{u}} + \overline{\rho'\boldsymbol{u}'\boldsymbol{u}'}) + \partial_x\bar{p} - \boldsymbol{\nabla}\cdot\bar{\boldsymbol{\tau}}_x^{\text{lam}} = 0.$$

The correlations of density and velocity fluctuations can be modeled as above. Collecting terms, one obtains

$$\partial_t(\bar{\rho}\bar{\boldsymbol{u}}) + \boldsymbol{\nabla}\cdot(\bar{\rho}\bar{\boldsymbol{u}}\bar{\boldsymbol{u}}) = -\partial_x\bar{p} + \boldsymbol{\nabla}\cdot(\bar{\boldsymbol{\tau}}_x^{\text{lam}} - \bar{\rho}\overline{\boldsymbol{u}'\boldsymbol{u}'} - \overline{\rho'\boldsymbol{u}'\boldsymbol{u}'}) - \partial_t(\overline{\rho'\boldsymbol{u}'}). \tag{17}$$

The average total stress thus contains a laminar and a turbulent part,

$$\bar{\boldsymbol{\tau}} = \boldsymbol{\tau}_{\text{lam}} - \bar{\rho}\overline{\boldsymbol{u}'\boldsymbol{u}'} - \overline{\rho'\boldsymbol{u}'\boldsymbol{u}'} \approx 2\bar{\rho}(\nu + \nu_t)\boldsymbol{D}, \tag{18}$$

with the strain rate tensor $\boldsymbol{D} := \frac{1}{2}\left[\boldsymbol{\nabla}\boldsymbol{u} + (\boldsymbol{\nabla}\boldsymbol{u})^{\mathrm{T}} - \frac{1}{3}\boldsymbol{\nabla}\cdot\boldsymbol{u}\mathbb{1}\right]$ and the turbulent viscosity ν_t, which, in turbulent flows, is much larger than the laminar viscosity ν. Investigating the terms $-\boldsymbol{\nabla}\cdot(\overline{\rho'\boldsymbol{u}'\boldsymbol{u}'})$ and $-\partial_t(\overline{\rho'\boldsymbol{u}'})$ is beyond the scope of this Note. However, from Eq. (17) it is clear there will be a term $\tau_{xz}(x, y, h_0 + h_1 + h_2, t)$ in the depth-averaged momentum balance equation, with both laminar and turbulent contributions that need to be modeled and included.

Entrainment rates In Eglit's original model, the entrainment *speeds* are modeled as the result of interfacial waves and instabilities, resulting in the following general expression:

$$V_{ij} = m_{ij}\|\boldsymbol{u}_j - \boldsymbol{u}_i\|\frac{\sqrt{\rho_i\rho_j}}{\rho_i + \rho_j}, \tag{19}$$

from which one arrives at the mass entrainment rates $q_{01} = \rho_0 V_{01}$, $q_{02} = \rho_0 V_{02}$, $q_{12} = \rho_1 V_{12}$, and $q_{a2} = \rho_a V_{a2}$. Across the bottom of the PSC, particles are assumed to settle out with the speed V_s, leading to the downward particle mass flux $q_p = c_2\rho_{\text{ice}}V_s$ and an (oppositely directed) air mass flux $-q_p\rho_a/\rho_{\text{ice}}$. They combine to the settling flux $q_s \approx (\rho_2 - \rho_a)V_s$ if one properly accounts for the upward speed q_s/ρ_0 of the interface. Where the PSC flows above the dense layer, i.e., $h_1 > 0$, this mass adds to the dense layer, $q_{21} = q_s$ while $q_{20} = 0$, otherwise it adds to the snow cover, hence $q_{21} = 0$ and $q_{20} = q_s$.

The assumption (19) does not appear well suited to quantifying entrainment from a cohesive granular mass. We suggest therefore to express the entrainment rates q_{01} and q_{02} by an equally simple formula in which the shear strength of the snow cover, τ_c, sets a threshold for entrainment (Issler & Jóhannesson, 2011; Issler, 2020). For conciseness, we define two indicator functions $\chi_1(h_1) := \Theta(h_1)$, $\chi_2(h_1) := 1 - \Theta(h_1)$, with the convention that $\Theta(0) = 0$. Then one can combine the formulas for q_{01} and q_{02} as

$$q_{0i} = \chi_i(h_1)\,\Theta(\|\boldsymbol{\tau}_{i0}\| - \tau_c)\frac{\|\boldsymbol{\tau}_{i0}\| - \tau_c}{\|\boldsymbol{u}_i\|}. \tag{20}$$

Using this formula for the entrainment rate will require a change in the formulation of the bed shear stresses, $\boldsymbol{\tau}_{10}$ and $\boldsymbol{\tau}_{20}$:

$$\|\boldsymbol{\tau}_{j0}\| = \min[\|\boldsymbol{\tau}_j(\boldsymbol{u}, h)\|, \tau_c], \tag{21}$$

where $\boldsymbol{\tau}_j(\boldsymbol{u}, h)$ is given by Eq. (12) for $j = 1$ and by Eq. (14) for $j = 2$ (with $i = 0$).

Turning attention to q_{a2}, one notes that Eq. (19) is linear in the relative velocity between layers and thus compatible with the entrainment hypothesis of Ellison & Turner (1959), which has been verified in a wide range of experiments. The density factor in Eq. (19) goes to 1/2 if $\rho_i = \rho_j$ and to $\sqrt{\rho_j/\rho_i} \ll 1$ if $\rho_i \ll \rho_j$. There is no dependence on the slope angle in Eq. (19) but experiments have consistently reported a quite pronounced slope dependence (Beghin & Olagne, 1991; Keller, 1996). Parker *et al.* (1986) capture the dependence of the entrainment rate of ambient fluid on the density difference and the slope angle by defining a bulk Richardson number (here written for the PSC) as

$$\mathrm{Ri}_b := \frac{(\rho_2 - \rho_a) g_z h_2}{\rho_a (\boldsymbol{u}_2 - \boldsymbol{u}_a)^2}. \tag{22}$$

(Ri_b is the inverse square of the densimetric Froude number.) The entrainment rate is parameterized as

$$q_{a2} = \frac{0.00153}{0.0204 + \mathrm{Ri}_b} \rho_a \|\boldsymbol{u}_2 - \boldsymbol{u}_a\|. \tag{23}$$

Different parameterizations have been proposed later, but they are qualitatively similar to Eq. (23). Equations (19) and (23) differ fundamentally. While Eq. (23) with its dependence on Ri_b and the slope angle appears to have a better physical foundation, it should be illuminating to compare the predictions of both formulations in actual simulations.

The interface between the dense flow and the PSC can be considered a boundary between two fluids of different density if the dense flow consists of sufficiently fine snow particles and is dilated enough for cohesion between snow balls to play a negligible role. Under these assumptions, the formula (19) should be a viable candidate for q_{12}, but the coefficient m_{12} should be chosen small enough because only a fraction of the mass in the dense layer consists of particles that are small enough to be suspended. Alternatively, a formula analogous to Eq. (23) multiplied by the weight ratio of sub-millimeter particles to all snow particles in the dense layer could be used because the the bulk Richardson number should be similarly relevant here. Given the central importance of q_{12} for the dynamics of the system, measuring and modeling this quantity will be one of the major challenges on the way to a realistic model of mixed avalanches.

2.5 Extensions of the Eglit model

The focus during model development will be to quickly create a running code. Nevertheless, there are some extensions of the model that could make it more suitable for practical

applications. If MoT-Voellmy is used as the code base, two of the three extensions mentioned below are already implemented (at least for the dense-flow layer) and can be taken over with few changes:

- *Spatially variable friction coefficients* make it possible to capture effects of variable snow temperature as a function of altitude. Direct comparison of the new model with RAMMS::Extended will require such a facility. This is possible in MoT-Voellmy—either constant values of μ and k are set, or their values at each computational cell are read in from specified raster files. There may be no need to adjust the parameters related to the PSC along the path.
- *Braking effect of forest:* For use in NAKSIN and in many hazard-mapping projects, it is important to assess the effect of existing forest on avalanche run-out. The formulas used in MoT-Voellmy would need minor adjustments to include the forces and moments exerted by and on the PSC.
- *Profile functions for density, velocity and pressure* are needed in many practical problems where PSCs are relevant. In depth-averaged models, profiles can be estimated if their shapes are known to be approximately constant within the flow and along the path. This was done, e.g., in SL-1D (Issler, 1998) by fitting measurements in a water tank (Keller, 1996) to quadratic polynomials $f(\zeta) = a + b\zeta + c\zeta^2$, where $\zeta = (z - h_0 - h_1)/h_2$. This approach could be carried over to the present case with minor adjustments.

3 Options for numerical implementation

In view of application in ongoing projects using NAKSIN, the main criteria for choosing a specific approach for programming a quasi-3D variant of the Eglit model are (i) code accuracy, (ii) code efficiency, (iii) compatibility with the NAKSIN framework, (iv) development time, and (v) "future-proofness" of the framework and maintainability.

Criterion (iv) can be addressed either by adapting an existing in-house or suitable open-source code for avalanches, or by using a general-purpose library for systems of hyperbolic differential equations. The two in-house codes that could be used in this context are MoT-Voellmy and VoellmyClaw, a code based on the ClawPack library for hyperbolic PDEs (Clawpack development team, 2021). Among the open-source codes are Titan2D (Pitman *et al.*, 2003), com1DFA (Oesterle *et al.*, 2021) from the AvaFrame project, and MassMov2D (Beguería *et al.*, 2009). GeoFlow_SPH (Pastor *et al.*, 2014) might also become available after discussion with its main author. Besides the ClawPack library, the development system ExaHyPE (Reinarz *et al.*, 2020) commands interest because it promises rapid code development combined with facilities to enable high-performance computing (HPC). Earlier experience with Titan2D and ClawPack has shown that these two libraries have steep learning curves because of limited documentation and parts consisting of hard-to-read Fortran-77 code.

Criterion (ii), code efficiency, will be of moderate importance in general hazard mapping work but becomes decisive in NAKSIN and applications to fully probabilistic quantitative risk assessment, where thousands of simulations may have to be run. According to our experience, MoT-Voellmy is by far the fastest code thanks to its simple numerics, coding in C and a few time-saving features like limiting the computational domain to the currently active area. Codes using Riemann solvers and higher-order discretization, like VoellmyClaw and Titan2D may achieve better stability and less diffusivity but at the price of about an order-of-magnitude longer computation times. Qualitative information about the dense-flow module in SAMOS-AT suggests that SPH codes also are slower than MoT-Voellmy if a sufficient number of "particles" are used. Interpreted codes like com1DFA or MassMov2D are at a further disadvantage in this respect.

The focus of ExaHyPE on HPC appears like the perfect answer to this requirement at first sight, yet there are several caveats: Snow avalanche problems in the context of hazard mapping are not very resource-intensive, a single core of a modern processor can handle them fairly quickly; dividing the problem into many small spatial blocks each associated with a core requires some initialization effort and increases the need for message-passing between cores. In NAKSIN, this is circumvented by working in parallel with many avalanche paths, each assigned to a specific processor. We therefore expect very little gain from ExaHyPE in this use case. Moreover, it needs to be confirmed whether an ExaHyPE code can be built that does not need recompiling whenever an input file or a model parameter are changed.

The existing NAKSIN code is adapted to MoT-Voellmy as the flow solver but can be modified to accommodate other solvers. It will nevertheless be an advantage if such a solver uses simply structured text files for setting up a run and reading its input data. We expect that the input and output routines of Titan2D, VoellmyClaw and GeoFlow_SPH would need partial or complete rewriting.

With regard to program maintenance and development, NGI has experienced serious problems with VoellmyClaw and BingClaw. A similar situation would probably arise with Titan2D. There is hope that com1DFA, GeoFlow_SPH and particularly MassMov2D would fare better in this respect, but this needs to be confirmed. MoT-Voellmy is a compact and fairly well-documented code and should therefore not create difficulties; a definitive verdict on this will come once other programmers beside the original author have worked with the code. However, the winner in this criterion should be ExaHyPE because the user codes seems to be limited to writing a simple file specifying the PDEs to be solved in almost mathematical notation and provide some configuration information. But it is unclear whether this still will apply if the problem geometry is not provided directly but through a DEM file indicated in a run configuration file.

The present trend in software development seems to be to use increasingly complex systems that generate substantial parts of the code automatically. This may boost efficiency of professional programmers but may come with a hefty price on the side of program efficiency and prevent avalanche experts who are not professional software developers from

developing a code further. ExaHyPE may be successful in making cutting-edge program design concepts usable and useful for non-professional software developers while using advanced numerical techniques behind the scenes and generating efficient and scalable code—this needs to be checked in more detail before a final decision is made. But even if this is confirmed, it remains to weigh carefully whether a simple and "old-fashioned" procedural code like MoT-Voellmy is more suitable in this specific context.

4 Conclusions

Eglit's two-layer model for mixed snow avalanches holds the promise of a substantial improvement of NGI's modeling capacity for snow avalanches with a moderate development effort and an acceptable slow-down of run-out calculations by an expected factor of about 3 compared to MoT-Voellmy. There are several arguments in favor of starting the development of a quasi-3D version of this model:

- The lack of a practically usable model for mixed avalanches has been felt increasingly in NGI's consulting activity and is one of the main gaps in NAKSIN.
- Eglit's model can be considered an extension of Voellmy-type models so that much of the experience gained with them will apply here as well.
- The model gives a consistent mathematical description of the basic physical laws.
- The model can be considered the minimum continuum model for mixed snow avalanches that accounts (explicitly or implicitly) for all essential processes of such flows. Thus, it offers an opportunity to gain practical experience with the modeling of mixed avalanches and to learn what other features could or should be incorporated in a more advanced model.
- The original quasi-2D model has been used with success in many simulations in the former Soviet Union, and there is some documentation available, including the choice of model parameters (almost all of it in Russian, however).
- Thanks to the relative simplicity of Eglit's model, development time can be kept to a minimum, independent of the choice of programming approach.

There is, however, no doubt that this is not a risk-free undertaking. The major sources of uncertainty are expected to be the following:

- Software development going beyond trivial modifications of a working code is almost always fraught with unforeseen difficulties.

- A two-layer system (or more correctly, a three-layer system including the snow cover) is inherently complex. If numerical instabilities arise, it may not be easy to understand their origin and to tame them.
- It will take a large number of simulations of different avalanche paths to fine-tune the model parameters to the point where plausible results can be obtained in a wide range of conditions, as is needed when using the code in NAKSIN. Particularly, the dependence of the model parameters on climatic conditions needs to be determined.

In summary, the Eglit model appears to be the most promising candidate for a rapid first step towards an advanced model of mixed snow avalanches. Its eight PDEs will be a part of the future model, potentially supplemented by further equations. It may be useful to modify some of the original closure relations already at this stage, notably regarding entrainment. Later on, further changes in the constitutive relations and source terms will likely be needed. But already with the original model, it should be possible to develop and test procedures for applying two-layer avalanche models in consulting or large-scale hazard mapping with NAKSIN.

Acknowledgements

This work was supported by a contract with Forsvarets Operative Hovedkvarter with the objective to create new and improved avalanche hazard indication maps for safe operations in potentially avalanche-prone terrain, and by the special grant for avalanche research at NGI from the Ministry of Petroleum and Energy, administrated by the Norwegian Water Resources and Energy Directorate (NVE). The author is grateful to Hervé Vicari for carefully checking the manuscript.

References

Bartelt, P., Buser, O., Vera Valero, C. & Bühler, Y. (2016). Configurational energy and the formation of mixed flowing/powder snow and ice avalanches. *Ann. Glaciol.* **57**(71), 179–188. doi:10.3189/2016AoG71A464.

Beghin, P. & Olagne, X. (1991). Experimental and theoretical study of the dynamics of powder snow avalanches. *Cold Regions Sci. Technol.* **19**, 317–326. doi:10.1016/0165-232x(91)90046-j.

Beguería, S., Van Asch, T. W. J., Malet, J.-P. & Gröndahl, S. (2009). A GIS-based numerical model for simulating the kinematics of mud and debris flows over complex terrain. *Nat. Haz. Earth Syst. Sci.* **9**, 1897–1909. doi:10.5194/nhess-9-1897-2009.

Clawpack development team (2021). Clawpack (Conservation Laws Package). Webpage. doi:10.17605/osf.io/kmw6h. URL http://www.clawpack.org. Last accessed: 2022-03-10.

Eglit, E. M. (1983). Some mathematical models of snow avalanches. *In:* Shahinpoor, M. (ed.), *Advances in the Mechanics and the Flow of Granular Materials*, vol. II, pp. 577–588. Trans Tech Publications, Clausthal-Zellerfeld, Germany, 1st edn..

Eglit, M. E. (1998). Mathematical and physical modelling of powder-snow avalanches in Russia. *Ann. Glaciol.* **26**, 281–284. doi:10.3189/1998AoG26-1-281-284.

Eglit, M. E., Yakubenko, A. & Zayko, J. (2020). A review of Russian snow avalanche models — from analytical solutions to novel 3D models. *Geosci.* **10**(2), 77. doi:10.3390/geosciences10020077.

Ellison, T. H. & Turner, J. S. (1959). Turbulent entrainment in stratified flows. *J. Fluid Mech.* **6**, 423–448.

Fukushima, Y. & Parker, G. (1990). Numerical simulation of powder-snow avalanches. *J. Glaciol.* **36**(123), 229–237.

Gauer, P. (1994). *Bewegung einer Staublawine längs eines Berghangs*. Masterarbeit, Fachbereich Mechanik (III), Technische Hochschule Darmstadt, Germany.

Grigoryan, S. S. (1979). A new law of friction and mechanism for large-scale avalanches and landslides. *Sov. Phys. Dokl.* **24**(2), 110–111.

Issler, D. (1998). Modelling of snow entrainment and deposition in powder-snow avalanches. *Ann. Glaciol.* **26**, 253–258. doi:10.3189/1998AoG26-1-253-258.

Issler, D. (2006). Curvature effects in depth-averaged flow models on arbitrary topography. NGI Report 20021048–14, Norwegian Geotechnical Institute, N–0806 Oslo, Norway.

Issler, D. (2020). Comments on "On a Continuum Model for Avalanche Flow and Its Simplified Variants" by S. S. Grigorian and A. V. Ostroumov. *Geosci.* **10**(3), 96. doi:10.3390/geosciences10030096.

Issler, D. & Gauer, P. (2008). Exploring the significance of the fluidized flow regime for avalanche hazard mapping. *Ann. Glaciol.* **49**(1), 193–198. doi:10.3189/172756408787814997.

Issler, D., Gleditsch Gisnås, K. & Domaas, U. (2020). Approaches to including climate and forest effects in avalanche hazard indication maps in Norway. Technical Note 20150457-10-TN, Norwegian Geotechnical Institute, Oslo, Norway. URL https://www.nve.no/media/10589/20150457-10-tn.pdf.

Issler, D., Jenkins, J. T. & McElwaine, J. N. (2018). Comments on avalanche flow models based on extensions of the concept of random kinetic energy. *J. Glaciol.* **64**(243), 148–164. doi:10.1017/jog.2017.62.

Issler, D. & Jóhannesson, T. (2011). Dynamically consistent entrainment and deposition rates in depth-averaged gravity mass flow models. NGI Technical Note 20110112-01-TN, Norwegian Geotechnical Institute, Oslo, Norway. doi:10.13140/RG.2.2.31327.71840.

Keller, S. (1996). Physikalische Simulation von Staublawinen – Experimente zur Dynamik im dreidimensionalen Auslauf. Mitteilung 141, Laboratory for Hydraulics, Hydrology and Glaciology, ETH Zurich, Zürich, Switzerland.

Kulikovskiy, A. G. & Sveshnikova, Y. I. (1977). Model'dlya rasheta dvizheniya pylevoy snezhnoy laviny (A model for calculating the motion of a powder-snow avalanche). *Mater. Glyatsiol. Issled.* **31**, 74–80. (In Russian).

Naaim, M. & Gurer, I. (1998). Two-phase numerical model of powder avalanche—theory and application. *Nat. Hazards* **117**, 129–145. doi:10.1023/A:1008002203275.

Nazarov, A. N. (1991). Mathematical modelling of a snow-powder avalanche in the framework of the equations of two-layer shallow water. *Izvest. Akad. Nauk SSSR, Mekh. Zhid. Gaza* **1991**(1), 84–90.

Oesterle, F., Tonnel, M., Wirbel, A. & Fischer, J.-T. (2021). com1DFAOrig: Original DFA-Kernel. Webpage. doi:https://zenodo.org/badge/latestdoi/281922740. URL https://docs.avaframe.org/en/latest/moduleCom1DFAOrig.html.

Parker, G., Fukushima, Y. & Pantin, H. M. (1986). Self-accelerating turbidity currents. *J. Fluid Mech.* **171**, 145–181. doi:10.1017/S0022112086001404.

Pastor, M., Blanc, T., Haddad, B., Petrone, S., Sanchez Morles, M. *et al.* (2014). Application of a SPH depth-integrated model to landslide run-out analysis. *Landslides* **11**, 793–812. doi:10.1007/s10346-014-0484-y.

Pitman, E. B., Nichita, C. C., Patra, A., Bauer, A., Sheridan, M. *et al.* (2003). Computing granular avalanches and landslides. *Phys. Fluids* **15**(12), 3638–3648. doi:10.1063/1.1614253.

Rastello, M. & Hopfinger, E. J. (2004). Sediment-entraining suspension clouds: a model of powder-snow avalanches. *J. Fluid Mech.* **509**, 181–206. doi:10.1017/S0022112004009322.

Rauter, M. & Köhler, A. (2020). Constraints on entrainment and deposition models in avalanche simulations from high-resolution radar data. *Geosci.* **10**(1), 9. doi:10.3390/geosciences10010009.

Reinarz, A., Charrier, D. E., Bader, M., Bovard, L., Dumbser, M. *et al.* (2020). ExaHyPE: An engine for parallel dynamically adaptive simulations of wave problems. *Comp. Phys. Comm.* **254**, 107,251. doi:10.1016/j.cpc.2020.107251.

Sampl, P. & Zwinger, T. (2004). Avalanche simulation with SAMOS. *Ann. Glaciol.* **38**, 393–398. doi:10.3189/172756404781814780.

Turnbull, B., McElwaine, J. N. & Ancey, C. J. (2007). The Kulikovskiy–Sveshnikova–Beghin model of powder snow avalanches: development and application. *J. Geophys. Res.* **112**, F0100. doi:10.1029/2006JF000489.

Voellmy, A. (1955). Über die Zerstörungskraft von Lawinen. *Schweiz. Bauztg.* **73**(12, 15, 17, 19), 159–165, 212–217, 246–249, 280–285.

Kontroll- og referanseside / Review and reference page

Dokumentinformasjon/*Document information*		
Dokumenttittel/*Document title* Outline of a Simple Model of Mixed Snow Avalanches		**Dokumentnr./*Document no.*** 20200017-10-TN
Dokumenttype/*Type of document* Teknisk notat / *Technical note*	**Oppdragsgiver/*Client*** Norges vassdrags- og energidirektorat (NVE)	**Dato/*Date*** 2023-08-24
Rettigheter til dokumentet iht kontrakt/*Proprietary rights to the document according to contract* ÅPEN: Skal tilgjengeliggjøres i åpent arkiv (BRAGE) / *OPEN: To be published in open archives (BRAGE)*		**Rev.nr. & dato/*Rev.no. & date*** 0 /
Distribusjon/Distribution		
Emneord/*Keywords* Snow avalanches, numerical modeling, mixed snow avalanches, Eglit model, entrainment functions		

Stedfesting/*Geographical information*	
Land, fylke/*Country* Norway	**Havområde/*Offshore area*** —
Kommune/*Municipality* —	**Feltnavn/*Field name*** —
Sted/*Location* —	**Sted/*Location*** —
Kartblad/*Map* —	**Felt, blokknr./*Field, Block No.*** —
UTM-koordinater/*UTM coordinates* **Sone:** 33N **Øst:** — **Nord:** —	**Koordinater/*Coordinates*** **Projeksjon, datum:** — **Øst:** ° ’ ” **Nord:** ° ’ ”

Dokumentkontroll/*Document control*
Kvalitetssikring i henhold til/*Quality assurance according to* NS-EN ISO9001

Rev.	**Revisjonsgrunnlag/*Reason for revision***	**Egenkontroll av/*Self review by:***	**Sidemanns-kontroll av/*Colleague review by:***	**Uavhengig kontroll av/*Independent review by:***	**Tverrfaglig kontroll av/*Interdisciplinary review by:***
0	Originaldokument	Dieter Issler 2022-05-18	Hervé Vicari 2022-03-18		

Dokument godkjent for utsendelse / *Document approved for release*	**Dato/*Date***	**Prosjektleder/*Project Manager***
	2023-08-24	Kjersti G. Gisnås

NGI (Norwegian Geotechnical Institute) is a leading international centre for research and consulting within the geosciences. NGI develops optimum solutions for society and offers expertise on the behaviour of soil, rock and snow and their interaction with the natural and built environment.

NGI works within the following sectors: Offshore energy – Building, Construction and Transportation – Natural Hazards – Environmental Engineering.

NGI is a private foundation with office and laboratory in Oslo, branch office in Trondheim and daughter companies in Houston, Texas, USA and in Perth, Western Australia.

www.ngi.no

NGI (Norges Geotekniske Institutt) er et internasjonalt ledende senter for forskning og rådgivning innen ingeniørrelaterte geofag. Vi tilbyr ekspertise om jord, berg og snø og deres påvirkning på miljøet, konstruksjoner og anlegg, og hvordan jord og berg kan benyttes som byggegrunn og byggemateriale.

Vi arbeider i følgende markeder: Offshore energi – Bygg, anlegg og samferdsel – Naturfare – Miljøteknologi.

NGI er en privat næringsdrivende stiftelse med kontor og laboratorier i Oslo, avdelingskontor i Trondheim og datterselskap i Houston, Texas, USA og i Perth, Western Australia.

www.ngi.no

OSLO
TRONDHEIM
HOUSTON
PERTH

NORWEGIAN GEOTECHNICAL INSTITUTE
NGI.NO

Main office
PO Box 3930 Ullevaal St.
NO-0806 Oslo
Norway

Trondheim office
PB. 5687 Torgarden
NO-7485 Trondheim
Norway

T (+47)22 02 30 00
F (+47)22 23 04 48
NGI@ngi.no

BIC NO. DNBANOKK
IBAN NO26 5096 0501 281
ORGANISATION NO.
958 254 318MVA

ISO 9001/14001
CERTIFIED BY BSI
FS 32989 / EMS 612006